DOI: 10.1002/ejic.200700779

The 1,1,3,3-Tetramethylguanidine–Borane Adduct: Theoretical Comparison of the Bonding Properties in Amine– and Guanidine–Borane Adducts

Oxana Ciobanu,[a] Simone Leingang,[a] Hubert Wadepohl,[a] and Hans-Jörg Himmel*[a]

Keywords: Boron hydrides / Dissociation energy / Guanidine adducts / Hydrogen bonding / Quantum chemical calculations

Herein we report on the synthesis and characterization of the adduct 1,1,3,3-tetramethylguanidine–borane, $H_3B{\cdot}N(H)C(NMe_2)_2$, and a general inspection of the bonding properties of guanidine adducts to BH_3. The new compound was characterized by its vibrational, NMR and mass spectra as well as single-crystal X-ray diffraction. Quantum chemical calculations match the experimental results. Particular attention was devoted to the evaluation of the dimeric assembly through H···H contacts of the molecules in the crystalline phase. The adduct is formed at 80 °C, but it also decomposes slowly at this temperature. The bonding properties in amine– and guanidine–borane adducts are compared in general on the basis of quantum chemical calculations carried out for several representative amine–borane adducts, namely $H_3B{\cdot}NH_3$, $H_3B{\cdot}NMe_3$ and $H_3B{\cdot}$quinuclidine, and guanidine–borane adducts, namely $H_3B{\cdot}N(H)C(NH_2)_2$, $H_3B{\cdot}N(H)C(NMe_2)_2$ and $H_3B{\cdot}$hppH, as well as the available experimental data for these species.

Introduction

Although amine adducts of BH_3 have been known for a long time, the interest in this class of compounds is renewed due to their potential applications in the fields of (1) hydrogen storage[1] and (2) dehydrocoupling and stoichiometric hydrogenation of olefins in the presence of a catalyst (homogeneous or heterogeneous catalysis).[2,3] Guanidines are generally stronger bases than amines,[4] and therefore their BH_3 adducts should exhibit increased stability. Nevertheless, surprisingly little is known about these species. All attempts by us and others to synthesize the parent compound $H_3B{\cdot}N(H)C(NMe_2)_2$ (**1**; Figure 1) have so far failed. Recently, we reported on the synthesis and structural characterization of the $H_3B{\cdot}$hppH adduct (**2**; Figure 1), where hppH = 1,3,4,6,7,8-hexahydro-2*H*-pyrimido[1,2-*a*]pyrimidine.[5] The experimental and quantum chemical analysis indicates the presence of significant *intramolecular* H···H bonding in **2**. Thus, two negatively polarized H atoms attached to the B atom interact with the positively polarized H atom attached to the N atom. Normally, borane–NH_3 adducts, or those of primary and secondary amines, interact through *intermolecular* H···H bonds in the crystalline phase. In ammonia–borane, $H_3B{\cdot}NH_3$ (**4**), intermolecular H···H contacts with shortest distances of 202 pm were measured by neutron diffraction techniques,[6] and these values are significantly shorter than the van der Waals distance of 240 pm. $H_3B{\cdot}$hppH eliminates dihydrogen gas at 110 °C to give the dinuclear B^{II} hydride $[HB(hpp)]_2$ featuring a direct B–B bond, which thus represents a new diborane(4) species (Scheme 1).[5]

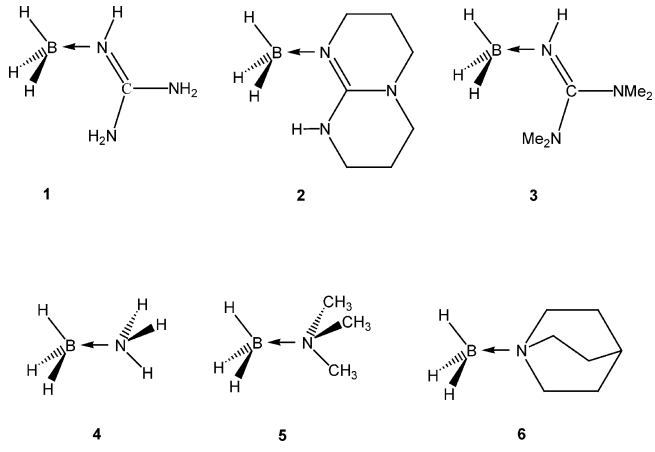

Figure 1. Lewis formula of compounds **1**–**6**.

Herein, we report on the synthesis and structural characterization of the new adduct $H_3B{\cdot}N(H)C(NMe_2)_2$ (**3**), which is only the second structurally characterized adduct of a guanidine derivative to BH_3. The Ga analogue $H_3Ga{\cdot}N(H)C(NMe_2)_2$[7] has already been synthesized previously and shown to feature an extremely short Ga–N distance for nitrogen base adducts to GaH_3 [198.81(19) pm was measured in the crystalline phase] and a dimeric assembly through intermolecular N–H···H–Ga contacts in the crystalline phase. First quantum chemical calculations with the use of the DFT method (BP86) and the SVP basis set returned a Ga–N bond length of 209.2 pm for an isolated

[a] Anorganisch-Chemisches Institut, Ruprecht-Karls-Universität Heidelberg,
Im Neuenheimer Feld 270, 69120 Heidelberg, Germany
E-mail: hans-jorg.himmel@aci.uni-heidelberg.de

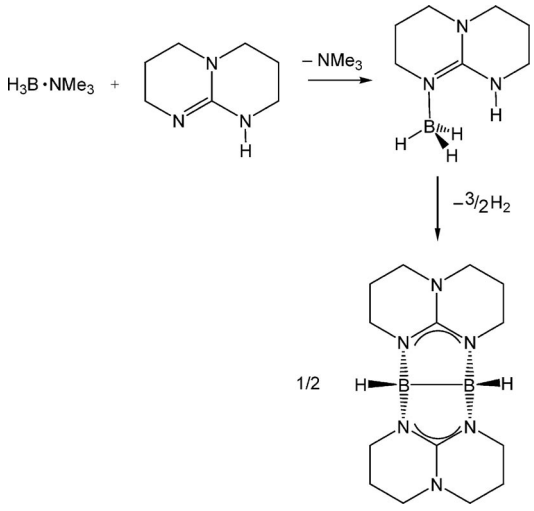

Scheme 1.

molecule,[7] which is a value that is more than 10 pm larger than that measured for the molecule in the crystalline phase. It is not the failure of the quantum chemical calculations that causes the seeming discrepancy between experiment and theory. Thus, large deviations were also reported between the B–N distances for amine adducts like $H_3B{\cdot}NH_3$ as measured by using X-ray diffraction in the crystalline phase and by using electron diffraction or rotational spectroscopy of the molecules in the gas phase.[8] For example, a distance of 156.4(6) pm was determined for $H_3B{\cdot}NH_3$ in the crystalline phase.[9] Rotational spectroscopy of gas-phase $H_3B{\cdot}NH_3$, however, returned a B–N distance of 165.8 pm.[10] The calculated and experimentally obtained gas-phase values are in good agreement, and therefore, the calculations should in general be compared with gas-phase data. However, the vapour pressure of the compounds is often not high enough to allow gas-phase analysis (which is also not often straightforward).

Despite of the short Ga–N bond length, $H_3Ga{\cdot}N(H)C(NMe_2)_2$ turned out to be thermally labile, and it decomposes at temperatures exceeding 330–350 °C.[7] A species with a central Ga_4N_4 unit was the only structurally characterized product of this decomposition, but unfortunately decomposition seems to occur through several channels.[7] The boron analogue will also be shown herein to be thermally labile, although the decomposition temperature is significantly higher. The accumulated experimental as well as quantum chemical data allow a detailed comparison of the bonding properties in amine– and guanidine–borane adducts. The calculated fragmentation and dissociation energies will be the centre of discussion (vide infra).

Results and Discussion

We start with the discussion of the synthetic routes leading to the borane adduct $H_3B{\cdot}N(H)C(NMe_2)_2$ (**3**) and the characterization of this molecule with the aid of several spectroscopic techniques and X-ray diffraction measurements. It follows a summary of the quantum chemical calculations performed for **3**. Finally, the B–N bonds in amine– and guanidine–BH_3 adducts are compared in detail. To this end, the B–N fragmentation and dissociation energies were calculated for several representatives to obtain information about the B–N bond strength.

Synthesis

For the synthesis of base adducts to the EH_3 hydrides (E = B or Ga), two routes have frequently been applied (Scheme 2). The first includes reaction of the HCl adduct of the guanidine base (L) with $LiEH_4$. The second represents a base exchange reaction, in which a base L′ such as NMe_3 is replaced by the stronger guanidine base L. Attack of the N=C bond is normally not an issue in this reaction. We used the second route to prepare 1,1,3,3-tetramethylguanidine–borane (**3**) in good yield. A solution of $H_3B{\cdot}NMe_3$ in toluene was added to a solution of 1,1,3,3-tetramethylguanidine, also in toluene. The reaction mixture was stirred for 18 h at 80 °C. The resulting solution was concentrated and subsequently stored at –20 °C to afford colourless crystals of **3**.

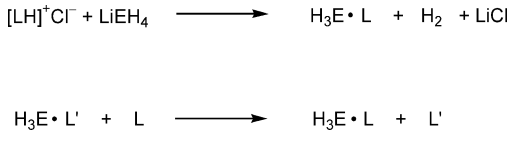

Scheme 2.

Spectroscopic Properties

IR Spectrum

Table 1 includes the wavenumbers of the strongest bands observed in the IR spectrum of solid **3** in CsI, and Figure 2 visualizes the spectrum in the region 4000–1000 cm^{-1}. A sharp band appears at 3337 cm^{-1} and can be assigned to the N–H stretch. For comparison, in the Ga homologue the stretching mode ν(N–H) was observed at 3317 cm^{-1}.[7] As discussed below, the molecules are assembled in dimeric units kept together through B–H···H–N contacts in the solid phase and maybe also in solution. These contacts weaken the N–H bond in addition to the effect of electron donation from the nitrogen base and therefore decrease the wavenumber of the stretching mode ν(N–H). A broader band with maxima at 2361 and 2291 cm^{-1} can be assigned to B–H stretches of **3**. The wavenumbers of the B–H stretching modes provide useful information about the amount of electron density donated from the base onto the BH_3 fragment. The increased electron density on the BH_3 group with respect to uncoordinated BH_3 leads to a decrease in the ν(B–H) frequencies. The stretches ν(BH_3) of free BH_3 that belong to the irreducible representation *e′* were reported to occur at 2601.57 cm^{-1} in the gas phase[11] and 2587.3 cm^{-1} in an Ar matrix.[12] In the case of $H_3B{\cdot}NMe_3$, the spectrum of the compound in solution

Table 1. Comparison between some experimentally observed and calculated IR properties of **3**.

Experimental [cm^{-1}]	Calculated $H_3B{\cdot}N(H)C(NMe_2)_2$ [cm^{-1}]	Calculated $[H_3B{\cdot}N(H)C(NMe_2)_2]_2$ [cm^{-1}]	Approximate description of molecular motion
3337	3582.9	3478.3/3474.0	ν(N–H)
2949	3175.8–2981.7	3171.4–3006.7	ν(C–H)
2365, 2291, 2259, 2239	2428.8–2381.6	2436.9–2341.8	ν(B–H)
1593	1647.8	1650.6/1641.3	ν(C=N)
	1586.2	1598.0/1593.3	δ_{ip}(N–H)
1453, 1433	1540.8–1453.3	1540.8–1456.5	δ(CH_3)
1159, 1072, 1042	1190.0–1176.1	1200.8–1193.0	δ(BH_3)
806	718.4	823.4–808.2	δ_{oop}(N–H)

showed bands at 2372 and 2270 cm^{-1} due to antisymmetric and symmetric ν(B–H) stretches,[13] respectively, and the corresponding bands in the spectrum of the molecule in solid Ar appeared at 2393/2275 [ν(^{10}B–H)], 2367/2270 cm^{-1} [ν(^{11}B–H)].[14]

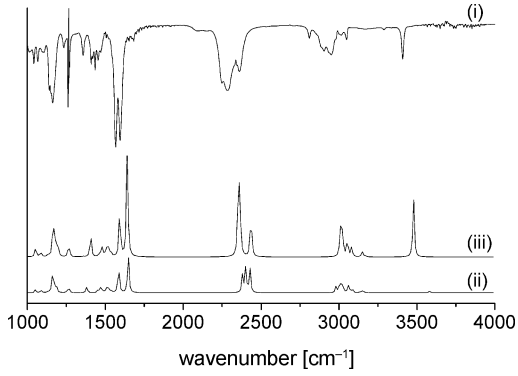

Figure 2. (i) Measured IR spectrum of solid **3** in CsI; (ii) calculated IR spectrum for individual molecules of **3**; (iii) calculated IR spectrum for dimeric assemblies of molecules of **3** interacting through N–H···H–B contacts. For the visualization of the calculated spectra, Lorenzian-type curves of 10 cm^{-1} half-width were used.

NMR Spectra (C_6D_6)

The resonance at δ_H = 4.61 ppm in the ^{1}H NMR spectrum of **3** belongs to the NH proton. It is shifted considerably with respect to the value in free guanidine, where δ_H(NH) = 5.27 ppm. In the case of $H_3B{\cdot}$hppH,[5] $H_3Ga{\cdot}N(H)C(NMe_2)_2$,[7] $Me_3Al{\cdot}N(H)C(NMe_2)_2$[15] and $Et_3Al{\cdot}N(H)C(NMe_2)_2$,[15] values of 3.34, 4.10, 4.40 and 5.20, respectively, were reported. A broad quartet centred at δ_H = 2.86 ppm (^1J = 95 Hz) can be assigned to the BH_3 protons. For comparison, in $H_3B{\cdot}NMe_3$, the BH_3 protons appear at δ_H = 2.40 ppm (^1J = 98 Hz). For $H_3B{\cdot}$hppH, a broad quartet at δ_H = 2.80 ppm (^1J = 93 Hz) was observed.[5] The protons of the four CH_3 groups in **3** show at δ_H = 2.51 and 1.72 ppm, and these positions are close to the values of 2.50 and 1.91 ppm reported for $H_3Ga{\cdot}N(H)C(NMe_2)_2$,[7] but they are shifted to larger values with respect to the free base, for which one obtains $\delta_H(CH_3)$ = 2.64 ppm. In the ^{11}B NMR spectrum, a quartet was detected at δ_B = –19.50 ppm (q, ^1J = 95 Hz). For comparison, the ^{11}B NMR quartet signal of $H_3B{\cdot}$hppH appears at δ_B = –19.15 ppm (q, ^1J = 93 Hz),[5] and in $H_3B{\cdot}NMe_3$, the ^{11}B NMR spectrum gives evidence for a quartet at δ_B = –7.27 (q, ^1J = 98 Hz).

Mass Spectrum

The spectrum shows strong peaks at *m*/*z* = 128.2 $[C_5H_{15}BN_3]^+$ and 126.2 $[C_5H_{13}BN_3]^+$, which can be assigned to ions formed with loss of one and three H atoms from the parent molecule, respectively. A small peak at *m*/*z* = 115.2 $[C_5H_{13}N_3]^+$ belongs to the free guanidine ligand. Elimination of CH_4 from $[C_5H_{15}BN_3]^+$ is responsible for the peak at *m*/*z* = 110.2. Loss of two methyl groups from the free guanidine base and of the NMe_2 group leads to signals at *m*/*z* = 85.2 and 71.2, respectively.

Crystal Structure

The structure of one molecule of **3** as derived from X-ray diffraction measurements is illustrated in Figure 3. Salient experimentally determined bond lengths and angles are included in Table 2. Like the Ga homologue,[7] **3** features a guanidine unit with a planar CN_3 core (the N–C–N angles sum to 360°). The B–N bond length measures 157.3(2) pm, and it is thus almost identical to that measured in crystalline $H_3B{\cdot}$hppH [157.5(2) pm][5] and significantly shorter than that found in crystalline $H_3B{\cdot}NMe_3$ [161.6(3) pm].[16] With 131.5 pm, the N=C bond is significantly shorter than the N–C bonds (134.6 and 135.8 pm) in the molecule. As

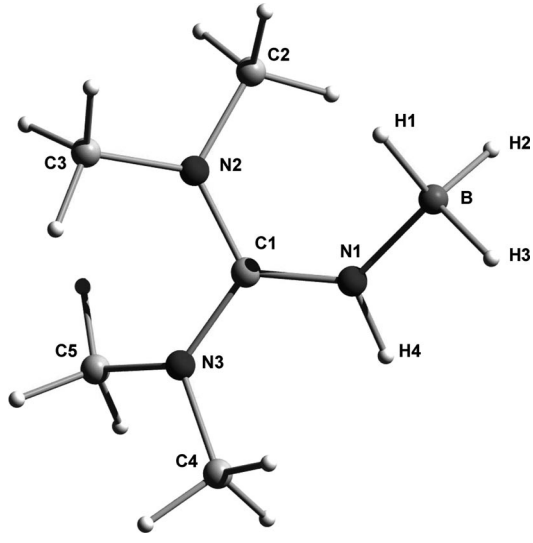

Figure 3. Structure of a $H_3B{\cdot}N(H)C(NMe_2)_2$ molecule in the crystalline phase as determined by X-ray diffraction.

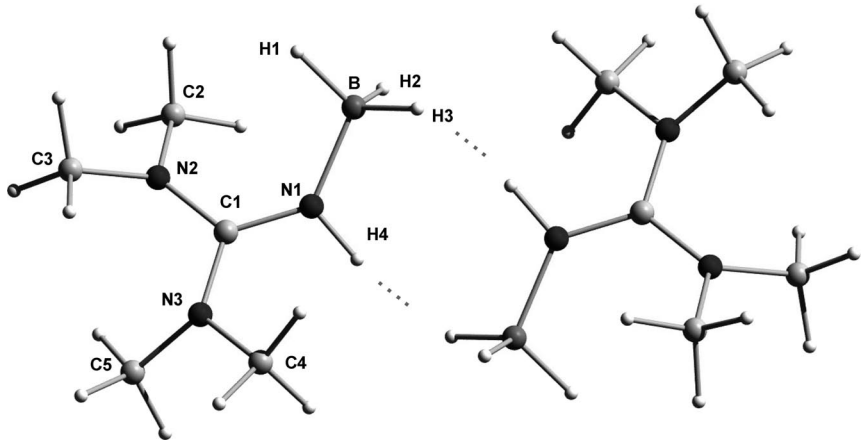

Figure 4. Dimeric assembly of **3** through N–H···H–B interactions in the crystalline phase.

already mentioned, the molecules are assembled in dimeric units in the crystalline phase, which are connected through B–H···H–N interactions (Figure 4). These H···H separations amount to 202 pm and are thus well within the range of 200–240 pm normally prescribed for unconventional hydrogen bonding of this sort.[17] By using normalized B/N–H distances, we obtained an even shorter B–H···H–N distance of 195 pm and B–H···H and H···H–N angles of 199.1° and 153.6°, respectively. For comparison, in $[H_2GaNH_2]_3$[18] and $[H_3AlN(H)Me_2]_2$[19] intermolecular H···H contacts of 197(2) and 192.5(1.9) pm, respectively, were measured.

Table 2. Selected intra–and intermolecular distances and angles for **3** in the crystal phase as determined by X-ray diffraction.[a]

Bond lengths [pm]			
B–N1	157.28(16)	C1–N3	135.82(13)
B–H1	110.2(15)	N2–C2	145.34(14)
B–H2	112.4(17)	N2–C3	144.90(15)
B–H3	112.3(14)	N3–C4	145.33(14)
N1–C1	131.54(13)	N3–C5	146.01(14)
N1–H4	92.6(16)		
C1–N2	134.57(13)	B–H···H–N[b]	202
Bond angles [°]			
N1–B–H1	109.7(7)	C1–N2–C2	121.91(10)
N1–B–H2	110.6(8)	C1–N2–C3	122.74(9)
N1–B–H3	105.3(7)	C2–N2–C3	115.35(10)
B–N1–C1	129.62(9)	C1–N3–C4	121.02(9)
B–N1–H4	117.0(9)	C1–N3–C5	121.74(9)
C1–N1–H4	112.5(9)	C4–N3–C5	114.59(9)
N1–C1–N2	121.30(9)		
N1–C1–N3	121.21(9)	B–H···H[b]	126.3
N2–C1–N3	117.48(9)	H···H–N[b]	154.7

[a] See Figures 3 and 4 for atom labelling. [b] Shortest intermolecular contacts.

Thermal Decomposition

Compound **3** was synthesized at 80 °C, but it also decomposes at this temperature (relatively fast in the solid state and very slowly in solution). Several experiments were carried out to analyze the decomposition pathway, but it should be admitted that we were not able to identify any decomposition products. Nevertheless, NMR spectroscopic studies gave useful first information. A sample of the solid product was heated for not more than 2 h to 80 °C. Afterwards, the NMR spectra were measured. The ^{11}B NMR (in C_6D_6) still showed a large quartet signal at δ = –19.58 ppm due to **3**, but quartet and triplet signals now appeared in addition at δ = –12.75/–11.81 and –3.65, respectively. In the ^1H NMR spectrum, new equally intense signals were observed at δ = 1.99 (s, CH_3) and 2.26 ppm (s, CH_3), which belong to the same molecule. Furthermore, a signal was detected at δ = 2.58 (s, CH_3) ppm. The decomposition products also gave rise to new signals at δ = 38.39, 51.21, 77.67 and 164.11 ppm in the ^{13}C NMR spectrum. Mass spectra were recorded of the gas-phase over a solid sample while increasing steadily the temperature from 25 °C to 500 °C at a pressure of 10^{-6} Torr. These spectra showed that (in vacuo) **3** partially sublimes without decomposition below 70 °C. However, a substantial fraction of the product decomposes during this process and remains as a solid. Further gas-phase species only occurred at temperatures between 410–500 °C. In the mass spectra recorded in this temperature range, the strongest signal was detected at *m*/*z* = 207.0 (indicating the presence of dinuclear species in the gas phase), but signals at higher values, *m*/*z* = 281, 355, 429, 503, were also found. One possible first decomposition product is the dinuclear species $\{H_2B[HNC(NMe_2)(NMe)]\}_2$, which is obtained from **3** upon CH_4 elimination and dimerization (Scheme 3). Quantum chemical calculations (vide infra) showed that such a reaction is highly exothermic. The observed value at *m*/*z* =107 corresponds to

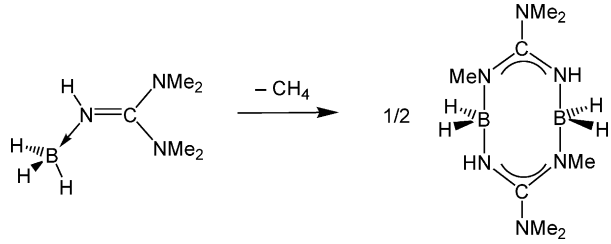

Scheme 3.

that of this dimer after removal of one methyl group and all four H atoms attached to the B atoms.

Quantum Chemical Calculations

Some parameters as calculated for **3** and its gallium homologue are compared with those determined by X-ray diffraction (XRD) in Tables 3 and 4 As expected, the calculated B–N distance is larger than the crystallographically derived one, although the difference is smaller than in the case of the Ga homologue (Table 4). Thus, the difference between the calculated and experimental (XRD) E–N distance (E = B or Ga) amounts to 2.7 pm for **3** but to 7.2 pm for $H_3Ga{\cdot}N(H)C(NMe_2)_2$. To test the accuracy of our calculations, we also compared the B–N distances calculated with B3LYP/6–311+G* with those measured for several other related compounds (Table 5). As anticipated, the agreement between the calculated distances and those measured for the gas-phase molecules is very pleasing, whereas the values measured by XRD come out too short. The largest discrepancy occurs for $H_3B{\cdot}NH_3$.

Table 3. Bond lengths (in pm) and bond angles (in °) as measured and calculated (B3LYP/6-311+G*) for **3**.

	Experimental	Calculated $H_3B{\cdot}N(H)C(NMe_2)_2$	Calculated $[H_3B{\cdot}N(H)C(NMe_2)_2]_2$
B–H1	110.2	121.4	121.2
B–H2	112.4	121.7	122.1
B–H3	112.3	121.9	122.5
B–N1	157.3	160.0	159.0
N1–H	92.6	101.1	101.7
N1=C	131.5	130.9	130.9
N2–C	134.6	136.4	136.8
N3–C	135.8	138.3	137.6
N1–C–N2	121.3	121.9	121.9
N1–C–N3	121.2	121.4	121.5
N2–C–N3	117.5	116.7	116.7
B–N1–C	129.6	130.7	130.0
H···H	202		189.1

Table 4. Bond lengths (in pm) and bond angles (in °) as measured and calculated (B3LYP/6–311+G*) for $H_3Ga{\cdot}N(H)C(NMe_2)_2$.

	Experimental	Calculated
Ga–H	149(4)/157(4)/161(4)	158.8/158.9/160.0
Ga–N1	198.8(2)	206.0
N1–H	78(3)	101.6
N1=C	131.6(3)	130.7
N2–C	134.7(3)	136.6
N3–C	136.0(3)	137.0
N1–C–N2	120.2(2)	120.9
N1–C–N3	122.2(2)	122.6
N2–C–N3	117.6(2)	116.5
Ga–N1–C	130.6(2)	130.2
H···H		197.9/197.5

Calculations were then carried out for a dimeric assembly of two molecules of **3** in which the molecules are allowed to interact though hydrogen–hydrogen contacts (Scheme 4). According to our B3LYP/6-311+G* calculations, the energy gain for formation of this dimeric assembly amounts to 43 kJ mol^{-1}, which implies that each of the N–H···H–B interactions is ca. 21 kJ mol^{-1} strong. This compares with a calculated (head-to-tail) dimerization energy of –60 kJ mol^{-1} (B3LYP/cc-pVDZ) or –63 kJ mol^{-1} (MP2/cc-pVDZ) for $H_3B{\cdot}NH_3$.[20] However, in the head-to-tail dimer $[H_3B{\cdot}NH_3]_2$, one N–H hydrogen atom interacts with two B–H hydrogen atoms, so that the bonding situation is slightly different. The zero-point corrected energy change for the reaction set out in Scheme 4 is –39 kJ mol^{-1}, and ΔG^0 = –5 kJ mol^{-1}. As expected, the N1–H and B–H3 bond lengths are slightly elongated in the dimeric assembly with respect to a single molecule of **3** as a result of the H···H interactions.

Table 5. B–N distances (in pm) as measured (solid and gas phases) and calculated (B3LYP/6–311+G*) for some guanidine [$HNC(NH_2)_2$, $HNC(NMe_2)_2$, hppH] and amine (NH_3, NMe_3, quinuclidine) adducts to BH_3.

	Experimental		Calculated
	Solid phase	Gas phase	
$H_3B{\cdot}N(H)C(NH_2)_2$ (**1**)	–	–	159.9
$H_3B{\cdot}$hppH (**2**)	157.5(2)[5]	–	160.2
$H_3B{\cdot}N(H)C(NMe_2)_2$ (**3**)	157.28(16)	–	160.7
$H_3B{\cdot}NH_3$ (**4**)	156.4(6)[9]	165.76(16)[25]	166.1
$H_3B{\cdot}NMe_3$ (**5**)	161.6[16]	163.7[26] 165.6(2)[27]	165.7
$H_3B{\cdot}$quinuclidine (**6**)	160.8(5)[24]	162.3(9)[24]	164.2

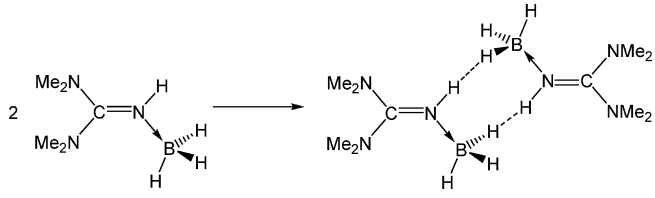

Scheme 4.

The vibrational properties are extremely sensitive to changes in the electronic properties. Of course, the presence of heavy mode coupling for the majority of modes makes any direct conclusion difficult. Nevertheless, a brief inspection discloses some important details (vide infra). Figure 2 compares the experimentally obtained spectrum of solid **3** in CsI with those calculated for (ii) individual molecules of **3** and (iii) dimeric assemblies of **3**. It can be directly seen that the spectrum calculated for the dimeric assembly fits better to the experimentally obtained one. Table 1 contains the calculated wavenumbers of some vibrational modes for which a straightforward description of molecular motion is possible. As anticipated, the wavenumber of the ν(N–H) mode calculated for the dimeric assembly is much lower than that calculated for individual molecules. From Figure 2 it can be seen that the relative intensity of the N–H stretching mode is calculated to be much higher in the dimeric assembly. Both the calculated wavenumber and relative intensity for the dimeric assembly are in better agreement with the experimental spectrum. In the same vein, the shapes of the bands and their wavenumbers in the region of the ν(B–H) modes fit better for the dimeric assembly than for individual molecules. This means that the IR spec-

tra are fully consistent with a dimeric assembly of **3** in the solid state.

Calculations were also carried out to shed light on the first step of the decomposition route of **3**. To this end, the thermodynamic properties of the reaction set out in Scheme 3 were calculated. Values of –307, –311 and –327 kJ mol^{-1} resulted for the energy change without and with ZPE corrections, respectively, and for ΔG^0. This is as expected, on the basis of the differences between the N–H and N–C bond dissociation energies, much higher than the H_2 elimination and dimerization of $H_3B{\cdot}N(H)C(NMe_2)_2$, for which we obtained ΔE, ΔE_{ZPE} and ΔG^0 values of –89, –128 and –125 kJ mol^{-1}, respectively (also using B3LYP/6-311+G*). For comparison, the corresponding reactions of $H_3B{\cdot}N(H)C(NH_2)_2$[21] and the amidine complex $H_3B{\cdot}N(H)C(H)(NH_2)$,[22] in which H_2 is released in place of CH_4, are associated with energy changes of –76 and –84 kJ mol^{-1}, respectively, according to previously calculated BP86/TZVPP estimates.

Analysis of the Bonding Properties in Amine– and Guanidine–BH_3 Adducts

In this section we compare the B–N bond strength in amine– and guanidine–BH_3 adducts. For such a comparison and from the numerous characterized amine–borane adducts, we chose three representatives, $H_3B{\cdot}NH_3$ (**4**), $H_3B{\cdot}NMe_3$ (**5**) and $H_3B{\cdot}$quinuclidine (**6**), because (1) extensive structural data is available for these compounds not only in the crystalline phase, but also in the gas phase and (2) the strength of the base increases steadily in the order $NH_3 < NMe_3 <$ quinuclidine (quinuclidine is already a strong amine base[23]). These amine–borane adducts will be compared with the three guanidine adducts $H_3B{\cdot}N(H)C(NH_2)_2$ (**1**), $H_3B{\cdot}N(H)C(NMe_2)_2$ (**3**) and $H_3B{\cdot}$hppH (**2**). In the case of parent compound **1**, the comparison must exclusively rely on quantum chemical data. All attempts to prepare this species failed and only an unknown noncrystalline white precipitate was recovered. For **3** (see above) and $H_3B{\cdot}$hppH (**2**),[5] X-ray diffraction measurements are available. Unfortunately, gas-phase measurements are likely to be hampered by the tendency of these compounds to eliminate either CH_4 (see above) or H_2[5] and dimerize at elevated temperature. The first observation is that the experimentally determined B–N distances in the crystalline phase do not show any clear trend (Table 5). The distances increase in the order (in pm) **4** (156.5)[9] < **3** (157.3) < **2** (157.5)[5] < **6** (160.9)[24] < **5** (161.6).[16] If $H_3B{\cdot}NH_3$ is treated as an exception, it could be concluded that the bond lengths in guanidine adducts are slightly shorter than those in amine adducts. This trend is supported by the calculated values, which show an increase in the order (in pm) **1** (159.9) < **2** (160.2) < **3** (160.7) < **6** (164.2) < **5** (165.7) < **4** (166.1). $H_3B{\cdot}NH_3$ now features the largest distance, which is in line with what is expected on the basis of the basicity order.[4,23] Because of the generally pleasing agreement between calculated and gas-phase values [165.76(16) pm for **4**,[25] 163.7(4)[26] or 165.6(2) pm[27] for **5** and 162.3(9) pm for **6**],[24] guanidine adducts (in the gas phase) indeed generally exhibit shorter distances than amine adducts.

Next, the B–N dissociation energies as calculated with B3LYP/6–311+G* were inspected (Table 6). The values were corrected for basis set superposition errors (BSSE), which are in the range 3–12 kJ mol^{-1}. As expected from the basicities, the dissociation energies for the three amine adducts follow the order (in kJ mol^{-1}) **4** (129) < **5** (139) < **6** (151). In the case of the guanidine adducts, the order (in kJ mol^{-1}) comes out to be **3** (138) < **1** (152) < **2** (166). In the case of **2**, the B–H···H–N contacts contribute to the bonding between the two fragments. It might be at first glance surprising that the dissociation energy of **3** is smaller than that of **6** and similar to that of **5**, although the B–N bond length in **3** is shorter in the crystalline phase and also according to the quantum chemical calculations. More importantly, the values do not reflect the basicity order.

To obtain a better estimate of the *intrinsic* B–N bond energies, the B–N fragmentation energies have to be considered (Table 6). The fragmentation energy differs from the dissociation energy in that relaxation of the fragments after bond cleavage is not included. Therefore, it is a better measure of the actual bond strength than the dissociation energy.[28] From Table 6 it can be seen that the relaxation energy, $\Delta E^{BSSE}{}_{relax}$, is the difference between the fragmentation and dissociation energies, and it contributes considerably to the dissociation energy. The relaxation energies of guanidine adducts come out to be larger than those of amine adducts. For example, the relaxation energies of $H_3B{\cdot}$hppH (**2**) and $H_3B{\cdot}$quinuclidine (**6**), amount to 89 and 66 kJ mol^{-1}, respectively. These large values cannot result from relaxation of the base (guanidine or amine) fragments,

Table 6. Fragmentation and dissociation (both in kJ mol^{-1}) without (ΔE_{frag} and ΔE_{diss}) and with BSSE corrections ($\Delta E^{BSSE}{}_{frag}$ and $\Delta E^{BSSE}{}_{diss}$) as well as relaxation energy $\Delta E^{BSSE}{}_{relax}(BH_3)$ and $\Delta E^{BSSE}{}_{relax}$(base) (summing up to the total relaxation energy $\Delta E^{BSSE}{}_{relax}$) as calculated for some guanidine [$HNC(NH_2)_2$, $HNC(NMe_2)_2$, hppH] and amine (NH_3, NMe_3, quinuclidine) adducts to BH_3.

Compound	ΔE_{frag}	ΔE_{diss}	$\Delta E^{BSSE}{}_{frag}$	$\Delta E^{BSSE}{}_{diss}$	$\Delta E^{BSSE}{}_{relax}$ (BH_3)	$\Delta E^{BSSE}{}_{relax}$ (base)
1	233.47	151.66	238.65	156.84	–73.78	–8.03
2	254.93	165.62	258.24	168.93	–81.36	–7.95
3	226.90	137.73	231.92	142.75	–72.83	–16.34
4	183.96	129.49	195.33	140.86	–54.45	–0.02
5	204.18	138.55	208.9	143.45	–59.11	–6.52
6	216.87	150.57	221.57	155.27	–61.73	–4.57

as the rigid skeleton of the base only allows a small amount of distortion. The largest contribution, therefore, must arise from relaxation of the BH_3 fragment. From Table 6 it can be seen that indeed for all adducts BH_3 relaxation into its planar D_{3h} symmetric energy minimum is the dominating contribution. The stronger the base, the more the H–B–H bond angles approach the tetrahedral angle of 109.4°. Hence, the average H–B–H bond angles are smaller in the guanidine adducts (111.5, 110.8 and 111.6° for **1**, **2** and **3**, respectively, compared with 113.6, 113.1 and 112.8° for **4**, **5** and **6**, respectively) and consequently the relaxation energy larger. The average H–B–H angle indeed appears to be a more reliable indicator of the B–N bond strength than the B–N bond length. However, the differences between the H–B–H angles are small.

Conclusions

A base exchange reaction between $H_3B{\cdot}NMe_3$ and 1,1,3,3-tetramethylguanidine, $HNC(NMe_2)_2$, affords the guanidine–borane adduct $H_3B{\cdot}N(H)C(NMe_2)_2$. In the crystalline phase, a dimeric assembly is observed in which the molecules are linked through two B–H···H–N contacts. Quantum chemical calculations (B3LYP/6–311+G*) predict an energy of 43 kJ mol^{-1} for these two contacts. The compound starts to decompose at 80 °C by a process that is relatively fast for the solid material and slow in (toluene) solution. The strength of the B–N bond in guanidine–borane adducts is accessed and compared to that of amine–borane adducts on the basis of quantum chemical calculations carried out for the compounds $H_3B{\cdot}N(H)C(NH_2)_2$, $H_3B{\cdot}N(H)C(NMe_2)_2$, $H_3B{\cdot}$hppH, $H_3B{\cdot}NH_3$, $H_3B{\cdot}NMe_3$ and $H_3B{\cdot}$quinuclidine, as well as experimental data (X-ray diffraction of the crystalline adducts and gas-phase measurements). Because relaxation of the BH_3 and base fragments is associated with a large energy gain, an adequate comparison has to include not only the dissociation, but also the fragmentation energies. As anticipated from the basicity order, the fragmentation energies are higher for guanidine than for amine adducts of BH_3. The B–N bond lengths turned out to be an unreliable criterion to judge the B–N bond strength. In addition to the large differences between the B–N bond lengths as determined from X-ray diffraction of the molecules in the solid state and gas phase or quantum chemical calculations, there is no direct correlation between the trends in the bond lengths and the fragmentation energies. The H–B–H angles correlate better with the fragmentation energies, although the differences in the angles between the adducts are small.

Experimental Section

General: All reactions were carried out under a dry nitrogen atmosphere by using standard Schlenk techniques. Toluene and other solvents were dried by standard methods and distilled before use. $H_3B{\cdot}NMe_3$ and $HNC(NMe_2)_2$ were purchased from Aldrich and used as delivered.

$H_3B{\cdot}N(H)C(NMe_2)_2$ (1): A solution of $H_3B{\cdot}NMe_3$ (0.42 g, 5.7 mmol) in toluene (30 mL) was slowly added by cannula to a stirred solution of 1,1,3,3-tetramethylguanidine (644 mg, 5.6 mmol) in toluene (20 mL). The reaction mixture was stirred for 18 h at 80 °C. The resulting solution was concentrated and stored at –20 °C to give colourless crystals of $H_3B{\cdot}N(H)C(NMe_2)_2$. ^{1}H NMR (400 MHz, C_6D_6): δ = 4.61 (s, 1 H, NH), 2.86 (br. q, ^1J = 95.0 Hz, 3 H, BH_3), 2.51 (s, 6 H, Me_2N), 1.72 (s, 6 H, Me_2N) ppm. ^{13}C NMR (100.55 MHz, C_6D_6): δ = 37.83 (CH_3), 39.63 (CH_3) ppm. ^{11}B NMR (128.30 MHz, C_6D_6): δ = –19.58 (q, ^1J = 95.0 Hz, BH_3) ppm. MS (EI+): *m*/*z* (%) = 128.2 (78) $[C_5H_{15}BN_3]^+$, 126.2 (100) $[C_5H_{13}BN_3]^+$, 115.2 (2) $[C_5H_{13}N_3]^+$, 110.2 (8) $[C_4H_9BN_3]^+$, 85.2 (24) $[C_3H_7N_3]^+$, 71.2 (31) $[C_3H_7N_2]^+$. Crystal data: $C_5H_{16}BN_3$, monoclinic, space group $P2_1/n$, a = 7.9154(10) Å, b = 9.2083(11) Å, c = 11.6854(15) Å, b = 104.279(2) °, V = 825.41(18) Å^3, Z = 4, m = 0.064 mm^{-1}, F(000) = 288. Reflections measured: 19791, independent: 2622 [R_{int} = 0.0565], index ranges $-11 < h \leq 11$, $0 \leq k \leq 13$, $0 \leq \lambda \leq 16$, θ range 2.8 to 31°. Intensity data were collected at 100 K with a Bruker AXS Smart 1000 CCD diffractometer (Mo-K_α radiation, graphite monochromator, λ = 0.71073 Å). Data were corrected for Lorentz, polarization and absorption effects (semiempirical, [SADABS],[29] max. and min. transmission factors 0.7460 and 0.5521). The structure was solved by direct methods[30] and refined by full-matrix least-squares methods based on F^2 with all measured unique reflections.[31] All non-hydrogen atoms were given anisotropic displacement parameters. All hydrogen atoms were located in difference Fourier syntheses and refined with individual isotropic displacement parameters. Final R values [$I > 2\sigma(I)$]: $R1$ = 0.0470, wR_2 = 0.1215, *GooF* = 1.062. CCDC-654679 contains the supplementary crystallographic data for this paper. These data can be obtained free of charge from The Cambridge Crystallographic Data Centre via www.ccdc.cam.ac.uk/data_request/cif.

Computational Details

All calculations were carried out with the aid of the Gaussian 98 guise of programs[32] by applying the hybrid DFT functional B3LYP[33,34] in combination with the 6-311+G* basis set.

Acknowledgments

The authors gratefully acknowledge financial support by the DFG (Deutsche Forschungsgemeinschaft) and the Fonds der Chemischen Industrie.

[1] See: F. H. Stephens, V. Pons, R. T. Baker, *Dalton Trans.* **2007**, 2613–2626.
[2] a) C. A. Jaska, I. Manners, *J. Am. Chem. Soc.* **2004**, *126*, 9776–9785; b) T. J. Clark, C. A. Russell, I. Manners, *J. Am. Chem. Soc.* **2006**, *128*, 9582–9583; c) T. J. Clark, K. Lee, I. Manners, *Chem. Eur. J.* **2006**, *12*, 8634–8648.
[3] Y. Luo, K. Ohno, *Organometallics* **2007**, *26*, 3597–3600.
[4] R. Schwesinger, *Chimia* **1985**, *39*, 269–272.
[5] O. Ciobanu, P. Roquette, S. Leingang, H. Wadepohl, J. Mautz, H.-J. Himmel, *Eur. J. Inorg. Chem.* **2007**, 4530–4534.
[6] W. T. Klooster, T. F. Koetzle, P. E. M. Siegbahn, T. B. Richardson, R. H. Crabtree, *J. Am. Chem. Soc.* **1999**, *121*, 6337–6343.
[7] A. R. Cowley, A. J. Downs, H.-J. Himmel, S. Marchant, J. A. Yeoman, *Dalton Trans.* **2005**, 1591–1597.
[8] See also the comparison with theoretical predictions: J. Volker, G. Frenking, *J. Chem. Soc. Chem. Commun.* **1994**, 1489–1490; and references cited therein.
[9] M. Bühl, T. Steinke, P. v. R. Schleyer, R. Boese, *Angew. Chem.* **1991**, *103*, 1179–1180; *Angew. Chem. Int. Ed. Engl.* **1991**, *30*, 1160–1161.

[10] L. R. Thorne, R. D. Suenram, F. J. Lovas, *J. Chem. Phys.* **1983**, *78*, 167–171.
[11] K. Kawaguchi, *J. Chem. Phys.* **1992**, *96*, 3411–3414.
[12] T. J. Tague Jr., L. Andrews, *J. Am. Chem. Soc.* **1994**, *116*, 4970–4976.
[13] C. F. Lane, *Chem. Rev.* **1976**, *76*, 773–800.
[14] J. D. Carpenter, B. S. Ault, *J. Phys. Chem.* **1991**, *95*, 3507–3511.
[15] R. Snaith, K. Wade, B. K. Wyatt, *J. Chem. Soc. A* **1970**, 380–383.
[16] A. Bakac, J. H. Espenson, *Inorg. Chem.* **1989**, *28*, 4319–4322.
[17] a) R. H. Crabtree, P. E. M. Siegbahn, O. Eisenstein, A. L. Rheingold, T. F. Koetzle, *Acc. Chem. Res.* **1996**, *29*, 348–354; b) W. T. Klooster, T. F. Koetzle, P. E. M. Siegbahn, T. B. Richardson, R. H. Crabtree, *J. Am. Chem. Soc.* **1999**, *121*, 6337–6343.
[18] a) J.-W. Hwang, J. P. Campbell, J. Kozubowski, S. A. Hanson, J. F. Evans, W. L. Gladfelter, *Chem. Mater.* **1995**, *7*, 517–525; b) J. P. Campbell, J.-W. Hwang, V. G. Young Jr., R. B. Von Dreele, C. J. Cramer, W. L. Gladfelter, *J. Am. Chem. Soc.* **1998**, *120*, 521–531.
[19] C. Y. Tang, R. A. Coxall, A. J. Downs, T. M. Greene, S. Parsons, *J. Chem. Soc. Dalton Trans.* **2001**, 2141–2147.
[20] C. J. Cramer, W. L. Gladfelter, *Inorg. Chem.* **1997**, *36*, 5358–5362.
[21] O. Ciobanu, H.-J. Himmel, *Eur. J. Inorg. Chem.* **2007**, 3565–3572.
[22] H.-J. Himmel, *Inorg. Chem.* **2007**, *46*, 6585–6593.
[23] A. J. Hoefnagel, M. A. Hoefnagel, B. M. Wepster, *J. Org. Chem.* **1981**, *46*, 4209–4211.
[24] F. Blockhuys, D. A. Wann, C. Van Alsenoy, H. E. Robertson, H.-J. Himmel, C. Y. Tang, A. R. Cowley, A. J. Downs, D. W. H. Rankin, *Dalton Trans.* **2007**, 1687–1696.
[25] L. R. Thorne, R. D. Suenram, F. J. Lovas, *J. Chem. Phys.* **1983**, *78*, 167–171.
[26] P. Cassoux, R. L. Kuczkowski, P. S. Bryan, R. C. Taylor, *Inorg. Chem.* **1975**, *14*, 126–129.
[27] K. Iijima, N. Adachi, S. Shibata, *Bull. Chem. Soc. Jpn.* **1984**, *57*, 3269–3273.
[28] H.-J. Himmel, H. Schnöckel, *Chem. Eur. J.* **2003**, *9*, 748–755.
[29] G. M. Sheldrick, *SADABS*-2004/1, Bruker AXS, **2004**.
[30] G. M. Sheldrick, *SHELXS-97*, University of Göttingen, **1997**.
[31] G. M. Sheldrick, *SHELXL-97*, University of Göttingen, **1997**.
[32] M. J. Frisch, G. W. Trucks, H. B. Schlegel, G. E. Scuseria, M. A. Robb, J. R. Cheeseman, V. G. Zakrzewski, J. A. Montgomery Jr., R. E. Stratmann, J. C. Burant, S. Dapprich, J. M. Millam, A. D. Daniels, K. N. Kudin, M. C. Strain, Ö. Farkas, J. Tomasi, V. Barone, M. Cossi, R. Cammi, B. Mennucci, C. Pomelli, C. Adamo, S. Clifford, J. Ochterski, G. A. Petersson, P. Y. Ayala, Q. Cui, K. Morokuma, P. Salvador, J. J. Dannenberg, D. K. Malick, A. D. Rabuck, K. Raghavachari, J. B. Foresman, J. Cioslowski, J. V. Ortiz, A. G. Baboul, B. B. Stefanov, G. Liu, A. Liashenko, P. Piskorz, I. Komáromi, R. Gomperts, R. L. Martin, D. J. Fox, T. Keith, M. A. Al-Laham, C. Y. Peng, A. Nanayakkara, M. Challacombe, P. M. W. Gill, B. Johnson, W. Chen, M. W. Wong, J. L. Andres, C. Gonzalez, M. Head-Gordon, E. S. Replogle, J. A. Pople, *Gaussian 98*, Gaussian, Inc., Pittsburgh, **1998**.
[33] A. D. Becke, *J. Chem. Phys.* **1993**, *98*, 5648–5652.
[34] a) C. Lee, W. Yang, R. G. Parr, *Phys. Rev. B* **1988**, *37*, 785–789; b) B. Miehlich, A. Savin, H. Stoll, H. Preuss, *Chem. Phys. Lett.* **1989**, *157*, 200–206.

Received: July 23, 2007
Published Online: November 7, 2007

